

**First Evidence of Direct CP Violation in Charmless Two-Body Decays of B_s^0 Mesons**R. Aaij *et al.**

(LHCb Collaboration)

(Received 29 February 2012; published 16 May 2012)

Using a data sample corresponding to an integrated luminosity of 0.35 fb^{-1} collected by LHCb in 2011, we report the first evidence of CP violation in the decays of B_s^0 mesons to $K^\pm \pi^\mp$ pairs, $A_{CP}(B_s^0 \rightarrow K\pi) = 0.27 \pm 0.08(\text{stat}) \pm 0.02(\text{syst})$, with a significance of 3.3σ . Furthermore, we report the most precise measurement of CP violation in the decays of B^0 mesons to $K^\pm \pi^\mp$ pairs, $A_{CP}(B^0 \rightarrow K\pi) = -0.088 \pm 0.011(\text{stat}) \pm 0.008(\text{syst})$, with a significance exceeding 6σ .

DOI: [10.1103/PhysRevLett.108.201601](https://doi.org/10.1103/PhysRevLett.108.201601)

PACS numbers: 11.30.Er, 13.25.Hw

The violation of CP symmetry, i.e., the noninvariance of fundamental forces under the combined action of the charge conjugation (C) and parity (P) transformations, is well established in the K^0 and B^0 meson systems [1–4]. Recent results from the LHCb collaboration have also provided evidence for CP violation in the decays of D^0 mesons [5]. Consequently, there now remains only one neutral heavy meson system, the B_s^0 , where CP violation has not yet been seen. All current experimental measurements of CP violation in the quark flavor sector are well described by the Cabibbo-Kobayashi-Maskawa mechanism [6,7] which is embedded in the framework of the standard model (SM). However, it is believed that the size of CP violation in the SM is not sufficient to account for the asymmetry between matter and antimatter in the Universe [8]; hence, additional sources of CP violation are being searched for as manifestations of physics beyond the SM.

In this Letter, we report measurements of direct CP violating asymmetries in $B^0 \rightarrow K^+ \pi^-$ and $B_s^0 \rightarrow K^- \pi^+$ decays using data collected with the LHCb detector. The inclusion of charge-conjugate modes is implied except in the asymmetry definitions. CP violation in charmless two-body B decays could potentially reveal the presence of physics beyond the SM [9–13], and has been extensively studied at the B factories and at the Tevatron [14–16]. The direct CP asymmetry in the $B_{(s)}^0$ decay rate to the final state $f_{(s)}$, with $f = K^+ \pi^-$ and $f_s = K^- \pi^+$, is defined as

$$A_{CP} = \Phi[\Gamma(\bar{B}_{(s)}^0 \rightarrow \bar{f}_{(s)}), \Gamma(B_{(s)}^0 \rightarrow f_{(s)})], \quad (1)$$

where $\Phi[X, Y] = (X - Y)/(X + Y)$ and $\bar{f}_{(s)}$ denotes the charge conjugate of $f_{(s)}$.

LHCb is a forward spectrometer covering the pseudorapidity range $2 < \eta < 5$, designed to perform flavor

physics measurements at the LHC. A detailed description of the detector can be found in Ref. [17]. The analysis is based on pp collision data collected in the first half of 2011 at a center-of-mass energy of 7 TeV, corresponding to an integrated luminosity of 0.35 fb^{-1} . The polarity of the LHCb magnetic field is reversed from time to time in order to partially cancel the effects of instrumental charge asymmetries, and about 0.15 fb^{-1} were acquired with one polarity and 0.20 fb^{-1} with the opposite polarity.

The LHCb trigger system comprises a hardware trigger followed by a high level trigger (HLT) implemented in software. The hadronic hardware trigger selects high transverse energy clusters in the hadronic calorimeter. A transverse energy threshold of 3.5 GeV has been adopted for the data set under study. The HLT first selects events with at least one large transverse momentum track characterized by a large impact parameter, and then uses algorithms to reconstruct D and B meson decays. Most of the events containing the decays under study have been acquired by means of a dedicated two-body HLT selection. To discriminate between signal and background events, this trigger selection imposes requirements on the quality of the online-reconstructed tracks (χ^2 per degree of freedom), their transverse momenta (p_T), and their impact parameters (d_{IP} , defined as the distance between the reconstructed trajectory of the track and the pp collision vertex), the distance of closest approach of the decay products of the B meson candidate (d_{CA}), its transverse momentum (p_T^B), its impact parameter (d_{IP}^B), and the decay time in its rest frame ($t_{\pi\pi}$, calculated assuming the decay into $\pi^+ \pi^-$). Only B candidates within the $\pi\pi$ invariant mass range 4.7–5.9 GeV/ c^2 are accepted. The $\pi\pi$ mass hypothesis is conventionally chosen to select all charmless two-body B decays using the same criteria.

Offline selection requirements are subsequently applied. Two sets of criteria have been optimized with the aim of minimizing the expected uncertainty either on $A_{CP}(B^0 \rightarrow K\pi)$ or on $A_{CP}(B_s^0 \rightarrow K\pi)$. In addition to more selective requirements on the kinematic variables already used in the HLT, two further requirements on the larger of the transverse momenta and of the impact

*Full author list given at the end of the article.

Published by the American Physical Society under the terms of the [Creative Commons Attribution 3.0 License](https://creativecommons.org/licenses/by/3.0/). Further distribution of this work must maintain attribution to the author(s) and the published article's title, journal citation, and DOI.

TABLE I. Summary of selection criteria adopted for the measurement of $A_{CP}(B^0 \rightarrow K\pi)$ and $A_{CP}(B_s^0 \rightarrow K\pi)$.

Variable	$A_{CP}(B^0 \rightarrow K\pi)$	$A_{CP}(B_s^0 \rightarrow K\pi)$
Track quality χ^2/ndf	<3	<3
Track p_T [GeV/c]	>1.1	>1.2
Track d_{IP} [mm]	>0.15	>0.20
$\max(p_T^K, p_T^\pi)$ [GeV/c]	>2.8	>3.0
$\max(d_{\text{IP}}^K, d_{\text{IP}}^\pi)$ [mm]	>0.3	>0.4
d_{CA} [mm]	<0.08	<0.08
p_T^B [GeV/c]	>2.2	>2.4
d_{IP}^B [mm]	<0.06	<0.06
$t_{\pi\pi}$ [ps]	>0.9	>1.5

parameters of the daughter tracks are applied. A summary of the two distinct sets of selection criteria is reported in Table I. In the case of $B_s^0 \rightarrow K\pi$ decays, a tighter selection is needed because the probability for a b quark to decay as $B_s^0 \rightarrow K\pi$ is about 14 times smaller than that to decay as $B^0 \rightarrow K\pi$ [18], and consequently a stronger rejection of combinatorial background (Comb. bkg.) is required. The two samples passing the event selection are then subdivided into different final states using the particle identification (PID) provided by the two ring-imaging Cherenkov (RICH) detectors. Again two sets of PID selection criteria are applied: a loose set optimized for the measurement of $A_{CP}(B^0 \rightarrow K\pi)$ and a tight set for that of $A_{CP}(B_s^0 \rightarrow K\pi)$.

To estimate the background from other two-body B decays with a misidentified pion or kaon (cross-feed background), the relative efficiencies of the RICH PID selection criteria must be determined. The high production rate of charged D^* mesons at the LHC and the kinematic characteristics of the $D^{*+} \rightarrow D^0(K^-\pi^+)\pi^+$ decay chain make such events an appropriate calibration sample for the PID of kaons and pions. In addition, for calibrating the response of the RICH system for protons, a sample of $\Lambda \rightarrow p\pi^-$ decays is used. PID information is not used to select either sample, as the selection of pure final states can be realized by means of kinematic criteria alone. The production and decay kinematics of the $D^0 \rightarrow K^-\pi^+$ and $\Lambda \rightarrow p\pi^-$ channels differ from those of the B decays under study. Since the RICH PID information is momentum dependent, the distributions obtained from calibration samples are reweighted according to the momentum distributions of B daughter tracks observed in data.

Unbinned maximum likelihood fits to the $K\pi$ mass spectra of the selected events are performed. The $B^0 \rightarrow K\pi$ and $B_s^0 \rightarrow K\pi$ signal components are described by single Gaussian functions convolved with a function which describes the effect of final state radiation on the mass line shape [19]. The background due to partially reconstructed three-body B decays is parametrized by means of an ARGUS function [20] convolved with a Gaussian resolution function. The combinatorial background is modeled by an exponential and the shapes of the cross-feed

backgrounds, mainly due to $B^0 \rightarrow \pi^+\pi^-$ and $B_s^0 \rightarrow K^+K^-$ decays with one misidentified particle in the final state, are obtained from Monte Carlo simulations. The $B^0 \rightarrow \pi^+\pi^-$ and $B_s^0 \rightarrow K^+K^-$ cross-feed background yields are determined from fits to the $\pi^+\pi^-$ and K^+K^- mass spectra, respectively, using events selected by the same offline selection as the signal and taking into account the appropriate PID efficiency factors. The $K^+\pi^-$ and $K^-\pi^+$ mass spectra for the events passing the two offline selections are shown in Fig. 1.

From the two mass fits we determine, respectively, the signal yields $N(B^0 \rightarrow K\pi) = 13\,250 \pm 150$ and $N(B_s^0 \rightarrow K\pi) = 314 \pm 27$, as well as the raw yield asymmetries $A_{\text{raw}}(B^0 \rightarrow K\pi) = -0.095 \pm 0.011$ and $A_{\text{raw}}(B_s^0 \rightarrow K\pi) = 0.28 \pm 0.08$, where the uncertainties are statistical only. In order to determine the CP asymmetries from the observed raw asymmetries, effects induced by the detector acceptance and event reconstruction, as well as due to strong interactions of final state particles with the detector material, need to be taken into account. Furthermore, the possible presence of a $B_{(s)}^0 - \bar{B}_{(s)}^0$ production asymmetry must also be considered. The CP asymmetry is related to the raw asymmetry by $A_{CP} = A_{\text{raw}} - A_\Delta$, where the correction A_Δ is defined as

$$A_\Delta(B_{(s)}^0 \rightarrow K\pi) = \zeta_{d(s)} A_D(K\pi) + \kappa_{d(s)} A_P(B_{(s)}^0), \quad (2)$$

where $\zeta_d = 1$ and $\zeta_s = -1$, following the sign convention for f and f_s in Eq. (1). The instrumental asymmetry $A_D(K\pi)$ is given in terms of the detection efficiencies ε_D of the charge-conjugate final states by $A_D(K\pi) = \Phi[\varepsilon_D(K^-\pi^+), \varepsilon_D(K^+\pi^-)]$, and the production asymmetry $A_P(B_{(s)}^0)$ is defined in terms of the $\bar{B}_{(s)}^0$ and $B_{(s)}^0$ production rates, $R(\bar{B}_{(s)}^0)$ and $R(B_{(s)}^0)$, as $A_P(B_{(s)}^0) = \Phi[R(\bar{B}_{(s)}^0), R(B_{(s)}^0)]$. The factor $\kappa_{d(s)}$ takes into account dilution due to neutral $B_{(s)}^0$ meson mixing, and is defined as

$$\kappa_{d(s)} = \frac{\int_0^\infty e^{-\Gamma_{d(s)}t} \cos(\Delta m_{d(s)}t) \varepsilon(B_{(s)}^0 \rightarrow K\pi; t) dt}{\int_0^\infty e^{-\Gamma_{d(s)}t} \cosh(\frac{\Delta\Gamma_{d(s)}}{2}t) \varepsilon(B_{(s)}^0 \rightarrow K\pi; t) dt}, \quad (3)$$

where $\varepsilon(B^0 \rightarrow K\pi; t)$ and $\varepsilon(B_s^0 \rightarrow K\pi; t)$ are the acceptances as functions of the decay time for the two reconstructed decays. To calculate κ_d and κ_s we assume that $\Delta\Gamma_d = 0$ and we use the world averages for Γ_d , Δm_d , Γ_s , Δm_s , and $\Delta\Gamma_s$ [4]. The shapes of the acceptance functions are parametrized using signal decay time distributions extracted from data. We obtain $\kappa_d = 0.303 \pm 0.005$ and $\kappa_s = -0.033 \pm 0.003$, where the uncertainties are statistical only. In contrast to κ_d , the factor κ_s is small, owing to the large B_s^0 oscillation frequency, thus leading to a negligible impact of a possible production asymmetry of B_s^0 mesons on the corresponding CP asymmetry measurement.

The instrumental charge asymmetry $A_D(K\pi)$ can be expressed in terms of two distinct contributions $A_D(K\pi) = A_I(K\pi) + \alpha(K\pi)A_R(K\pi)$, where $A_I(K\pi)$ is an asymmetry due to the different strong interaction cross

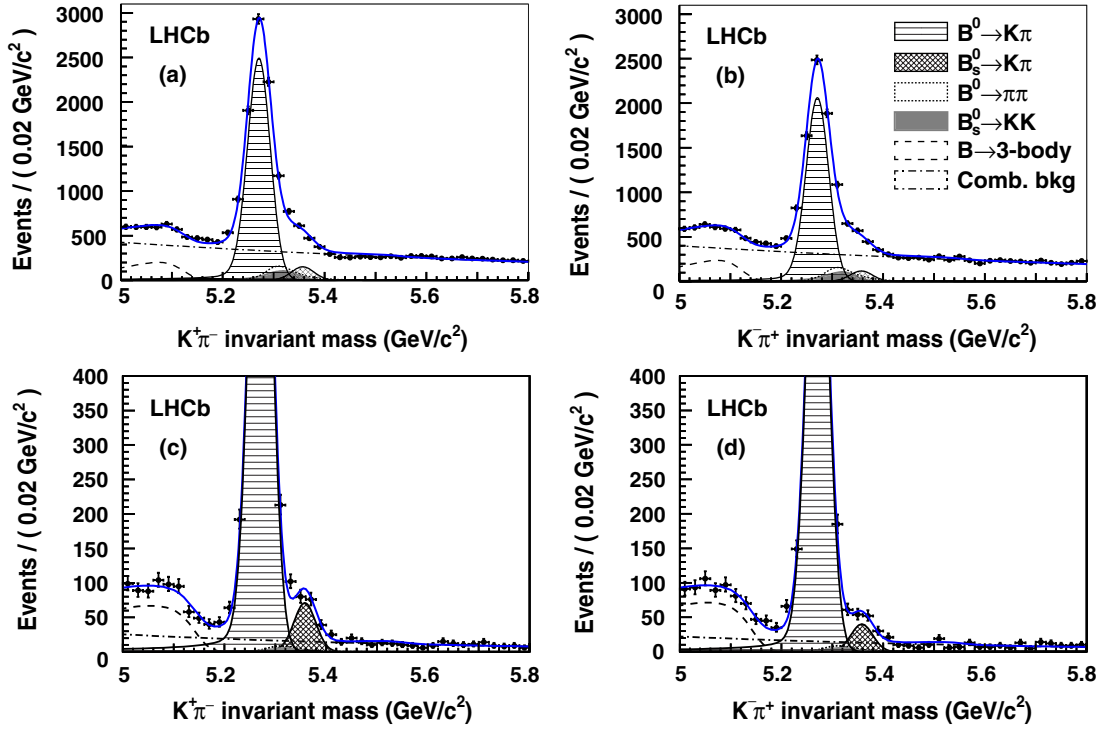


FIG. 1 (color online). Invariant $K\pi$ mass spectra obtained using the event selection adopted for the best sensitivity on (a), (b) $A_{CP}(B^0 \rightarrow K\pi)$ and (c), (d) $A_{CP}(B_s^0 \rightarrow K\pi)$. Plots (a) and (c) represent the $K^+\pi^-$ invariant mass whereas plots (b) and (d) represent the $K^-\pi^+$ invariant mass. The results of the unbinned maximum likelihood fits are overlaid. The main components contributing to the fit model are also shown.

sections with the detector material of $K^+\pi^-$ and $K^-\pi^+$ final state particles, and $A_R(K\pi)$ arises from the possible presence of a reconstruction or detection asymmetry. The quantity $A_I(K\pi)$ does not change its value by reversing the magnetic field, as the difference in the interaction lengths seen by the positive and negative particles for opposite polarities is small. By contrast, $A_R(K\pi)$ changes its sign when the magnetic field polarity is reversed. The factor $\alpha(K\pi)$ accounts for different signal yields in the data sets with opposite polarities, due to the different values of the corresponding integrated luminosities and to changing trigger conditions in the course of the run. It is estimated by using the yields of the largest decay mode, i.e., $B^0 \rightarrow K\pi$, determined from the mass fits applied to the two data sets separately. We obtain $\alpha(K\pi) = \Phi[N^{\text{up}}(B^0 \rightarrow K\pi), N^{\text{down}}(B^0 \rightarrow K\pi)] = -0.202 \pm 0.011$, where “up” and “down” denote the direction of the main component of the dipole field.

The instrumental asymmetries for the final state $K\pi$ are measured from data using large samples of tagged $D^{*+} \rightarrow D^0(K^-\pi^+)\pi^+$ and $D^{*+} \rightarrow D^0(K^-K^+)\pi^+$ decays, and untagged $D^0 \rightarrow K^-\pi^+$ decays. The combination of the integrated raw asymmetries of all these decay modes is necessary to disentangle the various contributions to the raw asymmetries of each mode, notably including the $K\pi$ instrumental asymmetry as well as that of the pion from the D^{*+} decay, and the production asymmetries of the D^{*+} and

D^0 mesons. In order to determine the raw asymmetry of the $D^0 \rightarrow K\pi$ decay, a maximum likelihood fit to the $K^-\pi^+$ and $K^+\pi^-$ mass spectra is performed. For the decays $D^{*+} \rightarrow D^0(K^-\pi^+)\pi^+$ and $D^{*+} \rightarrow D^0(K^-K^+)\pi^+$, we perform maximum likelihood fits to the discriminating variable $\delta m = M_{D^*} - M_{D^0}$, where M_{D^*} and M_{D^0} are the reconstructed D^* and D^0 invariant masses, respectively. Approximately 54×10^6 $D^0 \rightarrow K^-\pi^+$ decays, 7.5×10^6 $D^{*+} \rightarrow D^0(K^-\pi^+)\pi^+$ and 1.1×10^6 $D^{*+} \rightarrow D^0(K^-K^+)\pi^+$ decays are used. The mass distributions are shown in Figs. 2(a)–2(c). The $D^0 \rightarrow K^-\pi^+$ signal component is modeled as the sum of two Gaussian functions with the common mean convolved with a function accounting for final state radiation [19], on top of an exponential combinatorial background. The $D^{*+} \rightarrow D^0(K^-\pi^+)\pi^+$ and $D^{*+} \rightarrow D^0(K^-K^+)\pi^+$ signal components are modeled as the sum of two Gaussian functions convolved with a function taking account of the asymmetric shape of the measured distribution [5]. The background is described by an empirical function of the form $1 - e^{-(\delta m - \delta m_0)/\xi}$, where δm_0 and ξ are free parameters. Using the current world average of the integrated CP asymmetry for the $D^0 \rightarrow K^-K^+$ decay [21] and neglecting CP violation in the Cabibbo-favored $D^0 \rightarrow K^-\pi^+$ decay [22], from the raw yield asymmetries returned by the mass fits we determine $A_I(K\pi) = (-1.0 \pm 0.2) \times 10^{-2}$ and $A_R(K\pi) = (-1.8 \pm 0.2) \times 10^{-3}$, where the uncertainties are statistical only.

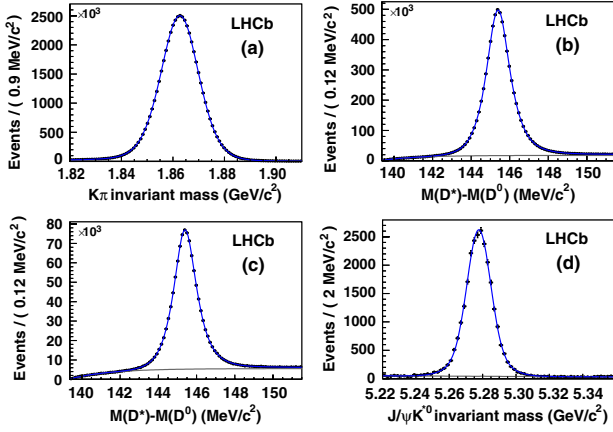


FIG. 2 (color online). Distributions of the invariant mass or invariant mass difference of (a) $D^0 \rightarrow K^- \pi^+$, (b) $D^{*+} \rightarrow D^0(K^- \pi^+) \pi^+$, (c) $D^{*+} \rightarrow D^0(K^- K^+) \pi^+$, and (d) $B^0 \rightarrow J/\psi(\mu^+ \mu^-) K^{*0}(K^+ \pi^-)$. The results of the maximum likelihood fits are overlaid.

The possible existence of a $B^0\text{-}\bar{B}^0$ production asymmetry is studied by reconstructing a sample of $B^0 \rightarrow J/\psi K^{*0}$ decays. CP violation in $b \rightarrow c\bar{c}s$ transitions, which is predicted in the SM to be at the 10^{-3} level [23], is neglected. The raw asymmetry $A_{\text{raw}}(B^0 \rightarrow J/\psi K^{*0})$ is determined from an unbinned maximum likelihood fit to the $J/\psi(\mu^+ \mu^-) K^{*0}(K^+ \pi^-)$ and $J/\psi(\mu^+ \mu^-) \bar{K}^{*0}(K^- \pi^+)$ mass spectra. The signal mass peak is modeled as the sum of two Gaussian functions with a common mean, whereas the combinatorial background is modeled by an exponential. The data sample contains approximately 25 400 $B^0 \rightarrow J/\psi K^{*0}$ decays. The mass distribution is shown in Fig. 2(d). To determine the production asymmetry we need to correct for the presence of instrumental asymmetries. Once the necessary corrections are applied, we obtain a value for the B^0 production asymmetry $A_P(B^0) = 0.010 \pm 0.013$, where the uncertainty is statistical only.

By using the instrumental and production asymmetries, the correction factor to the raw asymmetry $A_\Delta(B^0 \rightarrow K\pi) = -0.007 \pm 0.006$ is obtained. Since the B_s^0 meson has no valence quarks in common with those of the incident protons, its production asymmetry is expected to be smaller than for the B^0 , an expectation that is supported by hadronization models as discussed in Ref. [24]. Even conservatively assuming a value of the production asymmetry equal to that for the B^0 , owing to the small value of κ_s the effect of $A_P(B_s^0)$ is negligible, and we find $A_\Delta(B_s^0 \rightarrow K\pi) = 0.010 \pm 0.002$.

The systematic uncertainties on the asymmetries fall into the following main categories, related to (a) PID calibration, (b) modeling of the signal and background components in the maximum likelihood fits, and (c) instrumental and production asymmetries. Knowledge of PID efficiencies is necessary in this analysis to compute

the number of cross-feed background events affecting the mass fit of the $B^0 \rightarrow K\pi$ and $B_s^0 \rightarrow K\pi$ decay channels. In order to estimate the impact of imperfect PID calibration, we perform unbinned maximum likelihood fits after having altered the number of cross-feed background events present in the relevant mass spectra according to the systematic uncertainties affecting the PID efficiencies. An estimate of the uncertainty due to possible imperfections in the description of the final state radiation is determined by varying, over a wide range, the amount of emitted radiation [19] in the signal line shape parametrization. The possibility of an incorrect description of the core distribution in the signal mass model is investigated by replacing the single Gaussian with the sum of two Gaussian functions with a common mean. The impact of additional three-body B decays in the $K\pi$ spectrum, not accounted for in the baseline fit—namely $B \rightarrow \pi\pi\pi$ where one pion is missed in the reconstruction and another is misidentified as a kaon—is investigated. The mass line shape of this background component is determined from Monte Carlo simulations, and then the fit is repeated after having modified the baseline parametrization accordingly. For the modeling of the combinatorial background component, the fit is repeated using a first-order polynomial. Finally, for the case of the cross-feed backgrounds, two distinct systematic uncertainties are estimated: one due to a relative bias in the mass scale of the simulated distributions with respect to the signal distributions in data, and another accounting for the difference in mass resolution between simulation and data. All the shifts from the relevant baseline values are accounted for as systematic uncertainties. Differences in the kinematic properties of B decays with respect to the charm control samples, as well as different triggers and offline selections, are taken into account by introducing a systematic uncertainty on the values of the A_Δ corrections. This uncertainty dominates the total systematic uncertainty related to the instrumental and production asymmetries, and can be reduced in future measurements with a better understanding of the dependence of such asymmetries on the kinematics of selected signal and control samples. The systematic uncertainties for $A_{CP}(B^0 \rightarrow K\pi)$ and $A_{CP}(B_s^0 \rightarrow K\pi)$ are summarized in Table II.

In conclusion we obtain the following measurements of the CP asymmetries:

$$A_{CP}(B^0 \rightarrow K\pi) = -0.088 \pm 0.011(\text{stat}) \pm 0.008(\text{syst}),$$

and

$$A_{CP}(B_s^0 \rightarrow K\pi) = 0.27 \pm 0.08(\text{stat}) \pm 0.02(\text{syst}).$$

The result for $A_{CP}(B^0 \rightarrow K\pi)$ constitutes the most precise measurement available to date. It is in good agreement with the current world average provided by the Heavy Flavor Averaging Group $A_{CP}(B^0 \rightarrow K\pi) = -0.098^{+0.012}_{-0.011}$

TABLE II. Summary of systematic uncertainties on $A_{CP}(B^0 \rightarrow K\pi)$ and $A_{CP}(B_s^0 \rightarrow K\pi)$. The categories (a), (b), and (c) defined in the text are also indicated. The total systematic uncertainties given in the last row are obtained by summing the individual contributions in quadrature.

Systematic uncertainty	$A_{CP}(B^0 \rightarrow K\pi)$	$A_{CP}(B_s^0 \rightarrow K\pi)$
(a) PID calibration	0.0012	0.001
(b) Final state radiation	0.0026	0.010
(b) Signal model	0.0004	0.005
(b) Combinatorial background	0.0001	0.009
(b) 3-body background	0.0009	0.007
(b) Cross-feed background	0.0011	0.008
(c) Instr. and prod. asym. (A_Δ)	0.0078	0.005
Total	0.0084	0.019

[21]. Dividing the central value of $A_{CP}(B^0 \rightarrow K\pi)$ by the sum in quadrature of the statistical and systematic uncertainties, the significance of the measured deviation from zero exceeds 6σ , making this the first observation (greater than 5σ) of CP violation in the B meson sector at a hadron collider. The same significance computed for $A_{CP}(B_s^0 \rightarrow K\pi)$ is 3.3σ ; therefore, this is the first evidence for CP violation in the decays of B_s^0 mesons. The result for $A_{CP}(B_s^0 \rightarrow K\pi)$ is in agreement with the only measurement previously available [16].

We express our gratitude to our colleagues in the CERN accelerator departments for the excellent performance of the LHC. We thank the technical and administrative staff at CERN and at the LHCb institutes, and acknowledge support from the National Agencies: CAPES, CNPq, FAPERJ and FINEP (Brazil); CERN; NSFC (China); CNRS/IN2P3 (France); BMBF, DFG, HGF and MPG (Germany); SFI (Ireland); INFN (Italy); FOM and NWO (The Netherlands); SCSR (Poland); ANCS (Romania); MinES of Russia and Rosatom (Russia); MICINN, XuntaGal and GENCAT (Spain); SNSF and SER (Switzerland); NAS Ukraine (Ukraine); STFC (United Kingdom); NSF (USA). We also acknowledge the support received from the ERC under Contract No. FP7 and the Region of Auvergne.

- [1] J. H. Christenson, J. W. Cronin, V. L. Fitch, and R. Turlay, *Phys. Rev. Lett.* **13**, 138 (1964).
- [2] B. Aubert *et al.* (BABAR Collaboration), *Phys. Rev. Lett.* **87**, 091801 (2001).
- [3] K. Abe *et al.* (Belle Collaboration), *Phys. Rev. Lett.* **87**, 091802 (2001).
- [4] K. Nakamura *et al.* (Particle Data Group), *J. Phys. G* **37**, 075021 (2010).
- [5] R. Aaij *et al.* (LHCb Collaboration), *Phys. Rev. Lett.* **108**, 111602 (2012).
- [6] N. Cabibbo, *Phys. Rev. Lett.* **10**, 531 (1963).
- [7] M. Kobayashi and T. Maskawa, *Prog. Theor. Phys.* **49**, 652 (1973).
- [8] W.-S. Hou, *Chin. J. Phys. (Taipei)* **47**, 134 (2009), <http://psproc.phys.ntu.edu.tw/cjp/download.php?type=full&vol=47&num=2&page=134>.
- [9] R. Fleischer, *Phys. Lett. B* **459**, 306 (1999).
- [10] M. Gronau and J. L. Rosner, *Phys. Lett. B* **482**, 71 (2000).
- [11] H. J. Lipkin, *Phys. Lett. B* **621**, 126 (2005).
- [12] R. Fleischer, *Eur. Phys. J. C* **52**, 267 (2007).
- [13] R. Fleischer and R. Knegjens, *Eur. Phys. J. C* **71**, 1532 (2011).
- [14] B. Aubert *et al.* (BABAR Collaboration), [arXiv:0807.4226](https://arxiv.org/abs/0807.4226).
- [15] S. W. Lin *et al.* (Belle Collaboration), *Nature (London)* **452**, 332 (2008).
- [16] T. Aaltonen *et al.* (CDF Collaboration), *Phys. Rev. Lett.* **106**, 181802 (2011).
- [17] A. A. Alves, Jr *et al.* (LHCb Collaboration), *JINST* **3**, S08005 (2008).
- [18] T. Aaltonen *et al.* (CDF Collaboration), *Phys. Rev. Lett.* **103**, 031801 (2009).
- [19] E. Baracchini and G. Isidori, *Phys. Lett. B* **633**, 309 (2006).
- [20] H. Albrecht *et al.* (ARGUS Collaboration), *Phys. Lett. B* **229**, 304 (1989).
- [21] D. Asner *et al.* (Heavy Flavor Averaging Group), [arXiv:1010.1589](https://arxiv.org/abs/1010.1589).
- [22] S. Bianco, F. L. Fabbri, D. Benson, and I. Bigi, *Riv. Nuovo Cimento* **26N7**, 1 (2003).
- [23] W.-S. Hou, M. Nagashima, and A. Soddu, [arXiv:hep-ph/0605080](https://arxiv.org/abs/hep-ph/0605080).
- [24] R. W. Lambert, Ph.D. thesis, The University of Edinburgh 2008.

R. Aaij,³⁸ C. Abellan Beteta,^{33,a} B. Adeva,³⁴ M. Adinolfi,⁴³ C. Adrover,⁶ A. Affolder,⁴⁹ Z. Ajaltouni,⁵ J. Albrecht,³⁵ F. Alessio,³⁵ M. Alexander,⁴⁸ S. Ali,³⁸ G. Alkhazov,²⁷ P. Alvarez Cartelle,³⁴ A. A. Alves Jr,²² S. Amato,² Y. Amhis,³⁶ J. Anderson,³⁷ R. B. Appleby,⁵¹ O. Aquines Gutierrez,¹⁰ F. Archilli,^{18,35} L. Arrabito,⁵⁵ A. Artamonov,³² M. Artuso,^{53,35} E. Aslanides,⁶ G. Auriemma,^{22,b} S. Bachmann,¹¹ J. J. Back,⁴⁵ V. Balagura,^{28,35} W. Baldini,¹⁶ R. J. Barlow,⁵¹ C. Barschel,³⁵ S. Barsuk,⁷ W. Barter,⁴⁴ A. Bates,⁴⁸ C. Bauer,¹⁰ Th. Bauer,³⁸ A. Bay,³⁶ I. Bediaga,¹ S. Belogurov,²⁸ K. Belous,³² I. Belyaev,²⁸ E. Ben-Haim,⁸ M. Benayoun,⁸ G. Bencivenni,¹⁸ S. Benson,⁴⁷ J. Benton,⁴³ R. Bernet,³⁷ M.-O. Bettler,¹⁷ M. van Beuzekom,³⁸ A. Bien,¹¹ S. Bifani,¹² T. Bird,⁵¹ A. Bizzeti,^{17,c} P. M. Bjørnstad,⁵¹ T. Blake,³⁵ F. Blanc,³⁶ C. Blanks,⁵⁰ J. Blouw,¹¹ S. Blusk,⁵³ A. Bobrov,³¹ V. Bocci,²² A. Bondar,³¹ N. Bondar,²⁷ W. Bonivento,¹⁵ S. Borghi,^{48,51} A. Borgia,⁵³ T. J. V. Bowcock,⁴⁹ C. Bozzi,¹⁶ T. Brambach,⁹ J. van den Brand,³⁹ J. Bressieux,³⁶ D. Brett,⁵¹ M. Britsch,¹⁰ T. Britton,⁵³ N. H. Brook,⁴³ H. Brown,⁴⁹ A. Büchler-Germann,³⁷ I. Burducea,²⁶ A. Bursche,³⁷ J. Buytaert,³⁵ S. Cadetdu,¹⁵ O. Callot,⁷ M. Calvi,^{20,d} M. Calvo Gomez,^{33,a}

A. Camboni,³³ P. Campana,^{18,35} A. Carbone,¹⁴ G. Carboni,^{21,e} R. Cardinale,^{19,35,f} A. Cardini,¹⁵ L. Carson,⁵⁰ K. Carvalho Akiba,² G. Casse,⁴⁹ M. Cattaneo,³⁵ Ch. Cauet,⁹ M. Charles,⁵² Ph. Charpentier,³⁵ N. Chiapolini,³⁷ K. Ciba,³⁵ X. Cid Vidal,³⁴ G. Ciezarek,⁵⁰ P. E. L. Clarke,⁴⁷ M. Clemencic,³⁵ H. V. Cliff,⁴⁴ J. Closier,³⁵ C. Coca,²⁶ V. Coco,³⁸ J. Cogan,⁶ P. Collins,³⁵ A. Comerma-Montells,³³ A. Contu,⁵² A. Cook,⁴³ M. Coombes,⁴³ G. Corti,³⁵ B. Couturier,³⁵ G. A. Cowan,³⁶ R. Currie,⁴⁷ C. D'Ambrosio,³⁵ P. David,⁸ P. N. Y. David,³⁸ I. De Bonis,⁴ K. De Bruyn,³⁸ S. De Capua,^{21,e} M. De Cian,³⁷ F. De Lorenzi,¹² J. M. De Miranda,¹ L. De Paula,² P. De Simone,¹⁸ D. Decamp,⁴ M. Deckenhoff,⁹ H. Degaudenzi,^{36,35} L. Del Buono,⁸ C. Deplano,¹⁵ D. Derkach,^{14,35} O. Deschamps,⁵ F. Dettori,³⁹ J. Dickens,⁴⁴ H. Dijkstra,³⁵ P. Diniz Batista,¹ F. Domingo Bonal,^{33,a} S. Donleavy,⁴⁹ F. Dordei,¹¹ A. Dosil Suárez,³⁴ D. Dossett,⁴⁵ A. Dovbnaya,⁴⁰ F. Dupertuis,³⁶ R. Dzhelyadin,³² A. Dziurda,²³ S. Easo,⁴⁶ U. Egede,⁵⁰ V. Egorychev,²⁸ S. Eidelman,³¹ D. van Eijk,³⁸ F. Eisele,¹¹ S. Eisenhardt,⁴⁷ R. Ekelhof,⁹ L. Eklund,⁴⁸ Ch. Elsasser,³⁷ D. Elsby,⁴² D. Esperante Pereira,³⁴ A. Falabella,^{16,14,g} C. Färber,¹¹ G. Fardell,⁴⁷ C. Farinelli,³⁸ S. Farry,¹² V. Fave,³⁶ V. Fernandez Albor,³⁴ M. Ferro-Luzzi,³⁵ S. Filippov,³⁰ C. Fitzpatrick,⁴⁷ M. Fontana,¹⁰ F. Fontanelli,^{19,f} R. Forty,³⁵ O. Francisco,² M. Frank,³⁵ C. Frei,³⁵ M. Frosini,^{17,h} S. Furcas,²⁰ A. Gallas Torreira,³⁴ D. Galli,^{14,i} M. Gandelman,² P. Gandini,⁵² Y. Gao,³ J.-C. Garnier,³⁵ J. Garofoli,⁵³ J. Garra Tico,⁴⁴ L. Garrido,³³ D. Gascon,³³ C. Gaspar,³⁵ R. Gauld,⁵² N. Gauvin,³⁶ M. Gersabeck,³⁵ T. Gershon,^{45,35} Ph. Ghez,⁴ V. Gibson,⁴⁴ V. V. Gligorov,³⁵ C. Göbel,⁵⁴ D. Golubkov,²⁸ A. Golutvin,^{50,28,35} A. Gomes,² H. Gordon,⁵² M. Grabalosa Gándara,³³ R. Graciani Diaz,³³ L. A. Granado Cardoso,³⁵ E. Graugés,³³ G. Graziani,¹⁷ A. Grecu,²⁶ E. Greening,⁵² S. Gregson,⁴⁴ B. Gui,⁵³ E. Gushchin,³⁰ Yu. Guz,³² T. Gys,³⁵ C. Hadjivasiliou,⁵³ G. Haefeli,³⁶ C. Haen,³⁵ S. C. Haines,⁴⁴ T. Hampson,⁴³ S. Hansmann-Menzemer,¹¹ R. Harji,⁵⁰ N. Harnew,⁵² J. Harrison,⁵¹ P. F. Harrison,⁴⁵ T. Hartmann,⁵⁶ J. He,⁷ V. Heijne,³⁸ K. Hennessy,⁴⁹ P. Henrard,⁵ J. A. Hernando Morata,³⁴ E. van Herwijnen,³⁵ E. Hicks,⁴⁹ K. Holubyev,¹¹ P. Hopchev,⁴ W. Hulsbergen,³⁸ P. Hunt,⁵² T. Huse,⁴⁹ R. S. Huston,¹² D. Hutchcroft,⁴⁹ D. Hynds,⁴⁸ V. Iakovenko,⁴¹ P. Ilten,¹² J. Imong,⁴³ R. Jacobsson,³⁵ A. Jaeger,¹¹ M. Jahjah Hussein,⁵ E. Jans,³⁸ F. Jansen,³⁸ P. Jaton,³⁶ B. Jean-Marie,⁷ F. Jing,³ M. John,⁵² D. Johnson,⁵² C. R. Jones,⁴⁴ B. Jost,³⁵ M. Kaballo,⁹ S. Kandybei,⁴⁰ M. Karacson,³⁵ T. M. Karbach,⁹ J. Keaveney,¹² I. R. Kenyon,⁴² U. Kerzel,³⁵ T. Ketel,³⁹ A. Keune,³⁶ B. Khanji,⁶ Y. M. Kim,⁴⁷ M. Knecht,³⁶ R. F. Koopman,³⁹ P. Koppenburg,³⁸ M. Korolev,²⁹ A. Kozlinskiy,³⁸ L. Kravchuk,³⁰ K. Kreplin,¹¹ M. Krepes,⁴⁵ G. Krocker,¹¹ P. Krokovny,³¹ F. Kruse,⁹ K. Kruzelecki,³⁵ M. Kucharczyk,^{20,23,35,d} V. Kudryavtsev,³¹ T. Kvaratskheliya,^{28,35} V. N. La Thi,³⁶ D. Lacarrere,³⁵ G. Lafferty,⁵¹ A. Lai,¹⁵ D. Lambert,⁴⁷ R. W. Lambert,³⁹ E. Lanciotti,³⁵ G. Lanfranchi,¹⁸ C. Langenbruch,¹¹ T. Latham,⁴⁵ C. Lazzeroni,⁴² R. Le Gac,⁶ J. van Leerdam,³⁸ J.-P. Lees,⁴ R. Lefèvre,⁵ A. Leflat,^{29,35} J. Lefrançois,⁷ O. Leroy,⁶ T. Lesiak,²³ L. Li,³ L. Li Gioi,⁵ M. Lieng,⁹ M. Liles,⁴⁹ R. Lindner,³⁵ C. Linn,¹¹ B. Liu,³ G. Liu,³⁵ J. von Loeben,²⁰ J. H. Lopes,² E. Lopez Asamar,³³ N. Lopez-March,³⁶ H. Lu,³ J. Luisier,³⁶ A. Mac Raighne,⁴⁸ F. Machefert,⁷ I. V. Machikhiliyan,^{4,28} F. Maciuc,¹⁰ O. Maev,^{27,35} J. Magnin,¹ S. Malde,⁵² R. M. D. Mamunur,³⁵ G. Manca,^{15,j} G. Mancinelli,⁶ N. Mangiafave,⁴⁴ U. Marconi,¹⁴ R. Märki,³⁶ J. Marks,¹¹ G. Martellotti,²² A. Martens,⁸ L. Martin,⁵² A. Martín Sánchez,⁷ M. Martinelli,³⁸ D. Martinez Santos,³⁵ A. Massafferri,¹ Z. Mathe,¹² C. Matteuzzi,²⁰ M. Matveev,²⁷ E. Maurice,⁶ B. Maynard,⁵³ A. Mazurov,^{16,30,35} G. McGregor,⁵¹ R. McNulty,¹² M. Meissner,¹¹ M. Merk,³⁸ J. Merkel,⁹ S. Miglioranza,³⁵ D. A. Milanes,¹³ M.-N. Minard,⁴ J. Molina Rodriguez,⁵⁴ S. Monteil,⁵ D. Moran,¹² P. Morawski,²³ R. Mountain,⁵³ I. Mous,³⁸ F. Muheim,⁴⁷ K. Müller,³⁷ R. Muresan,²⁶ B. Muryn,²⁴ B. Muster,³⁶ J. Mylroie-Smith,⁴⁹ P. Naik,⁴³ T. Nakada,³⁶ R. Nandakumar,⁴⁶ I. Nasteva,¹ M. Needham,⁴⁷ N. Neufeld,³⁵ A. D. Nguyen,³⁶ C. Nguyen-Mau,^{36,k} M. Nicol,⁷ V. Niess,⁵ N. Nikitin,²⁹ T. Nikodem,¹¹ A. Nomerotski,^{52,35} A. Novoselov,³² A. Oblakowska-Mucha,²⁴ V. Obraztsov,³² S. Oggero,³⁸ S. Ogilvy,⁴⁸ O. Okhrimenko,⁴¹ R. Oldeman,^{15,35,j} M. Orlandea,²⁶ J. M. Otalora Goicochea,² P. Owen,⁵⁰ K. B. Pal,⁵³ J. Palacios,³⁷ A. Palano,^{13,l} M. Palutan,¹⁸ J. Panman,³⁵ A. Papanestis,⁴⁶ M. Pappagallo,⁴⁸ C. Parkes,⁵¹ C. J. Parkinson,⁵⁰ G. Passaleva,¹⁷ G. D. Patel,⁴⁹ M. Patel,⁵⁰ S. K. Paterson,⁵⁰ G. N. Patrick,⁴⁶ C. Patrignani,^{19,f} C. Pavel-Nicorescu,²⁶ A. Pazos Alvarez,³⁴ A. Pellegrino,³⁸ G. Penso,^{22,m} M. Pepe Altarelli,³⁵ S. Perazzini,^{14,i} D. L. Perego,^{20,d} E. Perez Trigo,³⁴ A. Pérez-Calero Yzquierdo,³³ P. Perret,⁵ M. Perrin-Terrin,⁶ G. Pessina,²⁰ A. Petrolini,^{19,f} A. Phan,⁵³ E. Picatoste Olloqui,³³ B. Pie Valls,³³ B. Pietrzyk,⁴ T. Pilař,⁴⁵ D. Pinci,²² R. Plackett,⁴⁸ S. Playfer,⁴⁷ M. Plo Casasus,³⁴ G. Polok,²³ A. Poluektov,^{45,31} E. Polcarpo,² D. Popov,¹⁰ B. Popovici,²⁶ C. Potterat,³³ A. Powell,⁵² J. Prisciandaro,³⁶ V. Pugatch,⁴¹ A. Puig Navarro,³³ W. Qian,⁵³ J. H. Rademacker,⁴³ B. Rakotomiaramanana,³⁶ M. S. Rangel,² I. Raniuk,⁴⁰ G. Raven,³⁹ S. Redford,⁵² M. M. Reid,⁴⁵ A. C. dos Reis,¹ S. Ricciardi,⁴⁶ A. Richards,⁵⁰ K. Rinnert,⁴⁹ D. A. Roa Romero,⁵ P. Robbe,⁷ E. Rodrigues,^{48,51} F. Rodrigues,² P. Rodriguez Perez,³⁴ G. J. Rogers,⁴⁴ S. Roiser,³⁵ V. Romanovsky,³² M. Rosello,^{33,a} J. Rouvinet,³⁶ T. Ruf,³⁵ H. Ruiz,³³ G. Sabatino,^{21,e}

J. J. Saborido Silva,³⁴ N. Sagidova,²⁷ P. Sail,⁴⁸ B. Saitta,^{15,j} C. Salzmann,³⁷ M. Sannino,^{19,f} R. Santacesaria,²² C. Santamarina Rios,³⁴ R. Santinelli,³⁵ E. Santovetti,^{21,e} M. Sapunov,⁶ A. Sarti,^{18,m} C. Satriano,^{22,b} A. Satta,²¹ M. Savrie,^{16,g} D. Savrina,²⁸ P. Schaack,⁵⁰ M. Schiller,³⁹ S. Schleich,⁹ M. Schlupp,⁹ M. Schmelling,¹⁰ B. Schmidt,³⁵ O. Schneider,³⁶ A. Schopper,³⁵ M.-H. Schune,⁷ R. Schwemmer,³⁵ B. Sciascia,¹⁸ A. Sciubba,^{18,m} M. Seco,³⁴ A. Semennikov,²⁸ K. Senderowska,²⁴ I. Sepp,⁵⁰ N. Serra,³⁷ J. Serrano,⁶ P. Seyfert,¹¹ M. Shapkin,³² I. Shapoval,^{40,35} P. Shatalov,²⁸ Y. Shcheglov,²⁷ T. Shears,⁴⁹ L. Shekhtman,³¹ O. Shevchenko,⁴⁰ V. Shevchenko,²⁸ A. Shires,⁵⁰ R. Silva Coutinho,⁴⁵ T. Skwarnicki,⁵³ N. A. Smith,⁴⁹ E. Smith,^{52,46} K. Sobczak,⁵ F. J. P. Soler,⁴⁸ A. Solomin,⁴³ F. Soomro,^{18,35} B. Souza De Paula,² B. Spaan,⁹ A. Sparkes,⁴⁷ P. Spradlin,⁴⁸ F. Stagni,³⁵ S. Stahl,¹¹ O. Steinkamp,³⁷ S. Stoica,²⁶ S. Stone,^{53,35} B. Storaci,³⁸ M. Straticiuc,²⁶ U. Straumann,³⁷ V. K. Subbiah,³⁵ S. Swientek,⁹ M. Szczekowski,²⁵ P. Szczypka,³⁶ T. Szumlak,²⁴ S. T'Jampens,⁴ E. Teodorescu,²⁶ F. Teubert,³⁵ C. Thomas,⁵² E. Thomas,³⁵ J. van Tilburg,¹¹ V. Tisserand,⁴ M. Tobin,³⁷ S. Tolk,³⁹ S. Topp-Joergensen,⁵² N. Torr,⁵² E. Tournefier,^{4,50} S. Tourneur,³⁶ M. T. Tran,³⁶ A. Tsaregorodtsev,⁶ N. Tuning,³⁸ M. Ubeda Garcia,³⁵ A. Ukleja,²⁵ P. Urquijo,⁵³ U. Uwer,¹¹ V. Vagnoni,¹⁴ G. Valenti,¹⁴ R. Vazquez Gomez,³³ P. Vazquez Regueiro,³⁴ S. Vecchi,¹⁶ J. J. Velthuis,⁴³ M. Veltri,^{17,n} B. Viaud,⁷ I. Videau,⁷ D. Vieira,² X. Vilasis-Cardona,^{33,a} J. Visniakov,³⁴ A. Vollhardt,³⁷ D. Volyanskyy,¹⁰ D. Voong,⁴³ A. Vorobyev,²⁷ V. Vorobyev,³¹ H. Voss,¹⁰ R. Waldi,⁵⁶ S. Wandernoth,¹¹ J. Wang,⁵³ D. R. Ward,⁴⁴ N. K. Watson,⁴² A. D. Webber,⁵¹ D. Websdale,⁵⁰ M. Whitehead,⁴⁵ D. Wiedner,¹¹ L. Wiggers,³⁸ G. Wilkinson,⁵² M. P. Williams,^{45,46} M. Williams,⁵⁰ F. F. Wilson,⁴⁶ J. Wishahi,⁹ M. Witek,²³ W. Witzeling,³⁵ S. A. Wotton,⁴⁴ K. Wyllie,³⁵ Y. Xie,⁴⁷ F. Xing,⁵² Z. Xing,⁵³ Z. Yang,³ R. Young,⁴⁷ O. Yushchenko,³² M. Zangoli,¹⁴ M. Zavertyaev,^{10,o} F. Zhang,³ L. Zhang,⁵³ W. C. Zhang,¹² Y. Zhang,³ A. Zhelezov,¹¹ L. Zhong,³ and A. Zvyagin³⁵

(LHCb Collaboration)

¹Centro Brasileiro de Pesquisas Físicas (CBPF), Rio de Janeiro, Brazil

²Universidade Federal do Rio de Janeiro (UFRJ), Rio de Janeiro, Brazil

³Center for High Energy Physics, Tsinghua University, Beijing, China

⁴LAPP, Université de Savoie, CNRS/IN2P3, Annecy-Le-Vieux, France

⁵Clermont Université, Université Blaise Pascal, CNRS/IN2P3, LPC, Clermont-Ferrand, France

⁶CPPM, Aix-Marseille Université, CNRS/IN2P3, Marseille, France

⁷LAL, Université Paris-Sud, CNRS/IN2P3, Orsay, France

⁸LPNHE, Université Pierre et Marie Curie, Université Paris Diderot, CNRS/IN2P3, Paris, France

⁹Fakultät Physik, Technische Universität Dortmund, Dortmund, Germany

¹⁰Max-Planck-Institut für Kernphysik (MPIK), Heidelberg, Germany

¹¹Physikalisches Institut, Ruprecht-Karls-Universität Heidelberg, Heidelberg, Germany

¹²School of Physics, University College Dublin, Dublin, Ireland

¹³Sezione INFN di Bari, Bari, Italy

¹⁴Sezione INFN di Bologna, Bologna, Italy

¹⁵Sezione INFN di Cagliari, Cagliari, Italy

¹⁶Sezione INFN di Ferrara, Ferrara, Italy

¹⁷Sezione INFN di Firenze, Firenze, Italy

¹⁸Laboratori Nazionali dell'INFN di Frascati, Frascati, Italy

¹⁹Sezione INFN di Genova, Genova, Italy

²⁰Sezione INFN di Milano Bicocca, Milano, Italy

²¹Sezione INFN di Roma Tor Vergata, Roma, Italy

²²Sezione INFN di Roma La Sapienza, Roma, Italy

²³Henryk Niewodniczanski Institute of Nuclear Physics Polish Academy of Sciences, Kraków, Poland

²⁴AGH University of Science and Technology, Kraków, Poland

²⁵Soltan Institute for Nuclear Studies, Warsaw, Poland

²⁶Horia Hulubei National Institute of Physics and Nuclear Engineering, Bucharest-Magurele, Romania

²⁷Petersburg Nuclear Physics Institute (PNPI), Gatchina, Russia

²⁸Institute of Theoretical and Experimental Physics (ITEP), Moscow, Russia

²⁹Institute of Nuclear Physics, Moscow State University (SINP MSU), Moscow, Russia

³⁰Institute for Nuclear Research of the Russian Academy of Sciences (INR RAN), Moscow, Russia

³¹Budker Institute of Nuclear Physics (SB RAS) and Novosibirsk State University, Novosibirsk, Russia

³²Institute for High Energy Physics (IHEP), Protvino, Russia

³³Universitat de Barcelona, Barcelona, Spain

³⁴Universidad de Santiago de Compostela, Santiago de Compostela, Spain

³⁵European Organization for Nuclear Research (CERN), Geneva, Switzerland

- ³⁶*Ecole Polytechnique Fédérale de Lausanne (EPFL), Lausanne, Switzerland*
³⁷*Physik-Institut, Universität Zürich, Zürich, Switzerland*
³⁸*Nikhef National Institute for Subatomic Physics, Amsterdam, The Netherlands*
³⁹*Nikhef National Institute for Subatomic Physics and VU University Amsterdam, Amsterdam, The Netherlands*
⁴⁰*NSC Kharkiv Institute of Physics and Technology (NSC KIPT), Kharkiv, Ukraine*
⁴¹*Institute for Nuclear Research of the National Academy of Sciences (KINR), Kyiv, Ukraine*
⁴²*University of Birmingham, Birmingham, United Kingdom*
⁴³*H. H. Wills Physics Laboratory, University of Bristol, Bristol, United Kingdom*
⁴⁴*Cavendish Laboratory, University of Cambridge, Cambridge, United Kingdom*
⁴⁵*Department of Physics, University of Warwick, Coventry, United Kingdom*
⁴⁶*STFC Rutherford Appleton Laboratory, Didcot, United Kingdom*
⁴⁷*School of Physics and Astronomy, University of Edinburgh, Edinburgh, United Kingdom*
⁴⁸*School of Physics and Astronomy, University of Glasgow, Glasgow, United Kingdom*
⁴⁹*Oliver Lodge Laboratory, University of Liverpool, Liverpool, United Kingdom*
⁵⁰*Imperial College London, London, United Kingdom*
⁵¹*School of Physics and Astronomy, University of Manchester, Manchester, United Kingdom*
⁵²*Department of Physics, University of Oxford, Oxford, United Kingdom*
⁵³*Syracuse University, Syracuse, New York, United States, USA*
⁵⁴*Pontifícia Universidade Católica do Rio de Janeiro (PUC-Rio), Rio de Janeiro, Brazil;
associated to Universidade Federal do Rio de Janeiro (UFRJ), Rio de Janeiro, Brazil*
⁵⁵*CC-IN2P3, CNRS/IN2P3, Lyon-Villeurbanne, France associated to CPPM, Aix-Marseille Université,
CNRS/IN2P3, Marseille, France*
⁵⁶*Institut für Physik, Universität Rostock, Rostock, Germany associated to Physikalisches Institut,
Ruprecht-Karls-Universität Heidelberg, Heidelberg, Germany*

^aLIFAELS, La Salle, Universitat Ramon Llull, Barcelona, Spain

^bUniversità della Basilicata, Potenza, Italy

^cUniversità di Modena e Reggio Emilia, Modena, Italy

^dUniversità di Milano Bicocca, Milano, Italy

^eUniversità di Roma Tor Vergata, Roma, Italy

^fUniversità di Genova, Genova, Italy

^gUniversità di Ferrara, Ferrara, Italy

^hUniversità di Firenze, Firenze, Italy

ⁱUniversità di Bologna, Bologna, Italy

^jUniversità di Cagliari, Cagliari, Italy

^kHanoi University of Science, Hanoi, Viet Nam

^lUniversità di Bari, Bari, Italy

^mUniversità di Roma La Sapienza, Roma, Italy

ⁿUniversità di Urbino, Urbino, Italy

^oP. N. Lebedev Physical Institute, Russian Academy of Science (LPI RAS), Moscow, Russia